Dissociation and Denaturation Equilibria and Kinetics of a Homogeneous Human Immunoglobulin Fab Fragment†

Elizabeth S. Rowe‡,§

ABSTRACT: The conformational equilibria and the kinetics of the approach to equilibrium of an IgG_1 myeloma (Wes) Fab fragment (SSFab) and its mildly reduced and *S*-carboxyamidomethylated derivative (RAFab) were studied as a function of guanidine hydrochloride concentration. The unimolecular denaturation of SSFab, the bimolecular denaturation of RAFab, and the denaturation of Wes L chain reported previously (Rowe, E. S., and Tanford, C., (1973), *Biochemistry 12,* 4822) are interpreted in terms of the domain structure and evaluated in terms of the thermodynamic stability of the protein and the covalent and noncovalent interactions among its subunits. The Fd–L interactions are found to be extremely strong and are maintained at concentrations of denaturant sufficient to denature the individual domains. It is shown that all of the data are consistent with a two region structure for Fab, one composed of the v_L and v_H domains, and the other composed of the c_L and c_H domains, so that there are two sites of noncovalent Fd–L interactions. One region, identified as the C region, is found to be 10^2–10^4 times more stable than the other; this difference in stability is attributed largely to a stronger and more extensive interaction between the domains of this region. The kinetics of the approach to equilibrium are found to be extremely slow in the center of the transitions, requiring up to a week for equilibration for RAFab, and several months for SSFab. This unusual kinetic behavior is shown to be due to the strong Fd–L interaction under conditions where the monomeric domains are unstable.

The Fab or antigen binding region of IgG[1] is composed of the N-terminal half of the H chain called Fd piece, and a whole L chain. Because both Fd and L chains contribute to antigen binding the interactions between these chains are an essential structural feature of IgG. The chains are held together primarily by noncovalent interactions; the single disulfide bond linking them can be easily reduced with no alteration in properties. After reduction of the interchain bond, the Fd and L chains can only be separated under denaturing conditions; after separation and renaturation, one or both of the chains assume a gross conformation different from that which it has in the associated state (Björk and Tanford, 1971c; Stevenson and Dorrington, 1970; Dorrington and Smith, 1972). Because of the difficulty of dissociating the chains, previous attempts to study the Fd–L interactions have been limited to qualitative dissociation (e.g., Zimmerman and Grey, 1972) or recombination studies (e.g., Mannik, 1967) under denaturing conditions using gel chromatography or electrophoresis to analyze yields (see Dorrington and Tanford, 1970). Some thermodynamic and kinetic experiments on the recombination of chains under native conditions have been reported (Dorrington and Kortan, 1974; Bigelow, et al., 1974); however, because of the high affinity of the association, equilibrium constants have not been measured. Thus little is known about the thermodynamics of the interactions between Fd and L chain.

Both the L chain and the Fd piece have been shown to be composed of two homology regions which are independently folded giving rise to four such globular domains in the Fab fragment; as shown by x-ray crystallographic data, these domains maintain their identity in the Fab structure (Poljak et al., 1973; Padlan et al., 1973). An understanding of the thermodynamic and functional behavior of this unique tertiary–quaternary structure in solution is essential for understanding antibody diversity and specificity.

Denaturation studies are capable of yielding information about the native state in terms of its cooperativity, intrinsic stability, and the nature of the forces responsible for maintaining that structure (Tanford, 1968, 1970). Denaturation studies of model proteins have provided some general principles which are useful in the analysis of more complicated proteins of biological interest. We have recently reported a denaturation study of an isolated L chain in which these principles were successfully applied to establish its domain structure in solution and determine some of its thermodynamic properties (Rowe and Tanford, 1973).

In order to dynamically study the domain structure of the Fab region in solution and relate the structural homologies to functional aspects of antibodies, in particular to the interactions between the H and L chains, we have undertaken a study of the conformational equilibria as a function of guanidine hydrochloride (Gdn·HCl)[2] concentration of the Fab fragment of a homogeneous human IgG_1 myeloma protein; this fragment is the simplest available system containing the features of interest. Previous attempts to study the Gdn·HCl denaturation of Fab fragments indicated, contrary to the behavior of model proteins in this solvent, that the denaturation of this protein species was either unusually

† From the Department of Biochemistry, Duke University Medical Center, Durham, North Carolina 27710. *Recieved July 8, 1975.* Supported in part by Research Grant AM-04576 from the National Institute of Arthritis and Metabolic Disease, U.S. Public Health Service.

‡ National Institutes of Health Predoctoral Fellow. This material was presented in partial fulfillment of the requirements for the degree of Doctor of Philosophy in the Department of Biochemistry, Duke University.

§ Present address: Department of Chemistry, Georgetown University, Washington, D.C. 20007.

[1] The nomenclature and abbreviations for the immunoglobulins and their subunits produced by reduction and proteolysis are those recommended by the World Health Organization (1964).

[2] Abbreviation used is: : Gdn·HCl, guanidine hydrochloride.

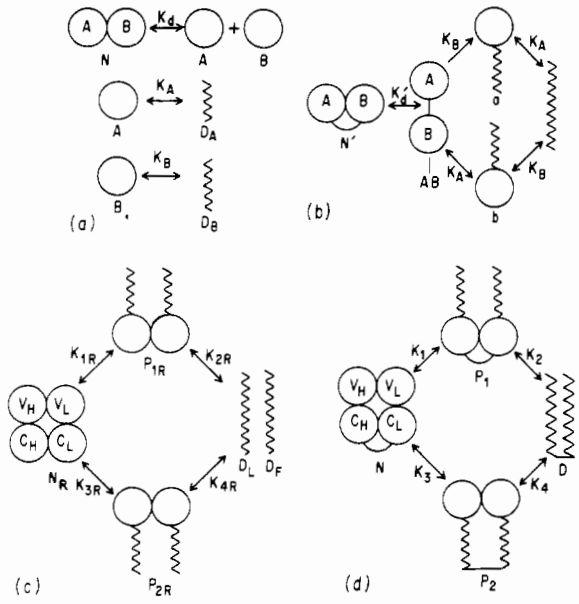

FIGURE 1: Denaturation models: (a) noncovalent dimer; (b) covalent dimer; (c) RAFab; (d) SSFab.

slow, or was not thermodynamically reversible; i.e., Gdn·HCl induced conformational changes were so slow that it could not be demonstrated that equilibrium was ever attained (Whitney, 1964; Cathou and Haber, 1967; Cathou and Werner, 1970). One of the objectives of the present investigation was to determine whether the apparently anomalous behavior of Fab fragment could be understood in terms of current concepts of the thermodynamics of proteins in solution, or whether these established principles apply only to the simplest proteins.

In the present report, the results of a study of the denaturation thermodynamics and kinetics of two forms of the Fab fragment from myeloma protein Wes, with and without its interchain disulfide bond, are reported. These results, and those for the isolated Wes L chain reported previously (Rowe and Tanford, 1973), are interpreted in terms of a self-consistent model which incorporates the features of the domain structure and the accepted principles of protein behavior. This interpretation, already presented in part (Rowe and Tanford, 1972), suggests some important implications concerning the functional properties of the unique tertiary–quaternary structure of the Fab region of antibodies.

Theoretical Background

In denaturation studies one measures the equilibrium between the native state N and the denatured state D in which, if Gdn·HCl is used as the denaturant, all the noncovalent interactions have been disrupted. If the native state N is a noncovalent dimer, e.g., an AB dimer such as shown in Figure 1a, the denaturation equilibrium is bimolecular and the equilibrium constant is

$$K_D = [D_A][D_B]/[N]$$

or, in terms of weight fraction of material in each state,

$$K_D = 4f_{DA}f_{DB}c_0/f_N \quad (1)$$

where c_0 is the total molar concentration in terms of dimer and f_x is the weight fraction of species X. As illustrated in Figure 1a, the denaturation of a dimer involves three processes, the bimolecular dissociation of the dimer, and the unimolecular unfolding of each monomer, so that

$$K_D = K_d K_A K_B \quad (2)$$

where

$$K_d = [A][B]/[N] = 4f_A f_B c_0/f_N$$

$$K_A = [D_A]/[A] = f_{DA}/f_A$$

and

$$K_B = [D_B]/[B] = f_{DB}/f_B$$

If we now consider the same dimer in which a covalent link between the monomers has been added, which has no effect on the intrinsic properties of the monomers or the interaction between them, but only prevents the monomers from becoming physically separated after the interaction between them is disrupted, the resulting processes are illustrated in Figure 1b. Here again, one can break the denaturation process into two unimolecular unfoldings and one unimolecular pseudodissociation, so that

$$K_D' = f_D/f_N' = K_d' K_A K_B \quad (3)$$

where $K_d' = f_{AB}/f_N'$, and the other symbols have the same meaning as before; the primes indicate quantities which are analogous to but different than those of the bimolecular process. In either case, if K_A and K_B can be measured independently, the dissociation constant K_d or the pseudodissociation constant K_d' can be obtained from eq 2 or 3.

If one is studying the denaturation of a protein which is a dimer under native conditions, the role of dissociation must be taken into consideration. One extreme case which may be observed is the case in which the denaturant disrupts the noncovalent interaction between the monomers at much lower concentration than required for unfolding the monomers, so that the denaturation transition is merely the unimolecular transition of a mixture of A and B monomers. In this case, identical results would be observed whether there were a covalent link between monomers or not. At the other extreme is the case in which the association between monomers is strong, such that dissociation occurs only as a consequence of unfolding, and the native state N is a dimer or pseudodimer throughout the transition (in eq 2 and 3 K_A, $K_B \gg 1$ during the unfolding transition). In this case, information about the interaction can be obtained from the denaturation study. In the latter case, in general a different result would be obtained for the noncovalent and the covalent dimer; the transition of the noncovalent dimer would be a function of protein concentration, whereas the covalent dimer transition would be independent of protein concentration.

The domain model of the Fab fragment of antibodies results in a considerably more complicated situation than that illustrated in Figure 1a and b. As shown in Figure 1c and d, the domain model implies the presence of four "monomer" units with pairwise noncovalent interactions between them in one dimension, and covalent links between them in another dimension. During unfolding of the Fab fragment, each of the two dimeric regions undergoes dissociation and denaturation of the monomers. Because the dissociation or pseudodissociation of the two halves are not independent, each has two equilibrium constants, depending on whether the neighboring dimeric region is associated or dissociated. Thus for this model there are four equations of the form in eq 2 or 3 for each of the forms, the covalent dimer and the noncovalent dimer.

These models provide a basis by which important infor-

mation about the Fab fragment can be obtained from a study of the denaturation equilibrium of the noncovalent Fab dimer in which the interchain SS bond is reduced and blocked, and the covalent dimer in which this bond is left intact. The simple model of Figure 1a and b can easily be distinguished from the domain model of Figure 1c and d by the presence of intermediate states such as shown in Figure 1c and d in which one dimeric region is native and associated while the other is dissociated and denatured. Interpretation of the denaturation data in terms of these models provides dynamic information about the domain structure in solution.

Materials and Methods

Proteins. Human serum from myeloma patient Wes was kindly donated by Dr. H. G. Kunkle; it was of the γ_1 subclass of IgG, and contained light chains of the κ type. The purification of the protein from the serum, and the separation of the chains were as described previously (Rowe and Tanford, 1973).

Fragments. SSFab (Fab fragment with intact interchain disulfide bond) and Fc fragment were obtained by digestion of the IgG myeloma protein with papain (Porter, 1959; Lebovitz et al., 1968). Separation of the digestion mixture was performed according to Edelman et al. (1968). The efficiency of the separation was confirmed by immunodiffusion studies using anti Fc and anti Fab antisera, which indicated no cross contamination of the Fab and Fc fractions. The molecular weight of the Wes Fab chains, and the efficiency of papain cleavage were checked simultaneously by gel filtration in 6 M Gdn·HCl of a fully reduced and carboxymethylated sample of Wes Fab on a calibrated column of 6% agarose according to Fish et al. (1969). By this technique it was found that 95% of the material eluted as a single peak corresponding to a molecular weight of 24 000, with less than 5% of material having a molecular weight of 50 000, probably representing uncleaved heavy chains. The presence of the interchain disulfide bond was established by sedimentation equilibrium measurements in which a molecular weight of 46 000 was obtained for Wes Fab both in 0.1 M NaCl and in 6 M Gdn·HCl.

RAFab (mildly reduced and *S*-carboxamidomethylated Wes Fab) was prepared by the method of Fleishman et al. (1962), as modified by Björk and Tanford (1971a), from Wes SSFab. The successful selective reduction of the interchain disulfide bond was confirmed by gel filtration of a sample, with no further reduction, in a calibrated 6% agarose 6 M Gdn·HCl column. 95% of the material eluted with an apparent molecular weight of 18 000 which is consistent with L chain containing its disulfide loops.

Protein concentrations were determined by optical density measurements using $E_{1\text{ cm},279}(1\%)$ 13.5 for Wes Fab, as determined by dry weight measurements. Other extinction coefficients were, for Wes IgG, $E_{1\text{ cm},279}(1\%)$ 13.0, for Wes L, $E_{1\text{ cm},280}(1\%)$ 10.8, and for Wes H, $E_{1\text{ cm},280}(1\%)$ 14.4 (Green, 1973). The extinction coefficient for Fc was calculated from those of Wes Fab and Wes IgG to be 12.0.

Guanidine Hydrochloride. Guanidine hydrochloride was UHP Gu·HCl Lot 777, purchased from Heico, Inc. Stock solutions were filtered and used without further purification. The concentrations of stock solutions were determined by measuring the index of refraction at 5892 Å and determining the concentration from the data of Keilly and Harrington (1960).

Experimental Procedures. The optical rotation measurements were performed using a Cary 60 recording spectropolarimeter equipped with sample temperature control. Equilibrium and kinetic experiments were performed as previously described (Rowe and Tanford, 1973) except that for kinetic experiments of long duration, periodic rather than continuous measurements were made. In addition, control experiments were performed to eliminate the possibility that prolonged exposure of partially unfolded proteins to the high intensity Xenon lamp of the Cary 60 led to peptide breakage (Wilson and Foster, 1970) under the conditions of our kinetic experiments. It was found that irradiation in the Cary 60 of unfolded protein at 239.6 nm for up to at least 24 h had no effect on the results obtained or the ability of the unfolded protein to regain the native conformation.

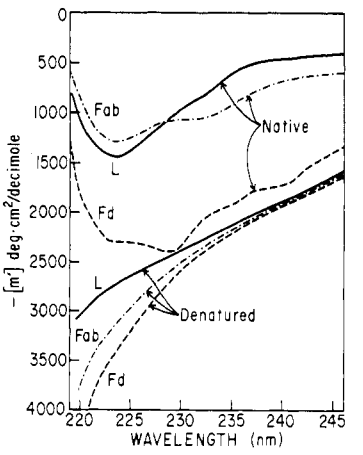

FIGURE 2: ORD spectra of native and denatured Fab and L chain, and ORD spectra of native and denatured Fd, calculated as described in the text.

Results

In Figure 2 are shown the optical rotatory dispersion (ORD) spectra of Wes Fab in the native state N and in the denatured state D. The spectra of SSFab and RAFab in both states were identical throughout the spectral region shown, confirming that the selective reduction of the interchain disulfide bond in RAFab had no effect on its gross conformation. Also shown for comparison are the spectra of native and denatured Wes L chain. The spectra shown for native Fd piece is a theoretical one calculated from the spectra of Wes H chain and Wes Fc fragment by the relation

$$[m']_{Fd,native} = 2[m']_H - [m']_{Fc}$$

The calculated spectrum of denatured Fd was obtained from the relation

$$[m']_{Fd,denatured} = 2[m']_{Fab,denatured} - [m']_{L,denatured}$$

The spectra of the denatured states are characteristic of cross-linked randomly coiled polypeptides, as was their behavior on gel filtration in 6 M Gdn·HCl.

The transition from the native state N to the denatured state D was followed by measuring the optical rotation (OR) at 239.6 and 220 nm as a function of Gdn·HCl concentration. The fractional contributions of dissociation, L chain denaturation, and Fd denaturation to the transition of Fab at these wavelengths can be calculated from the spectra to be:

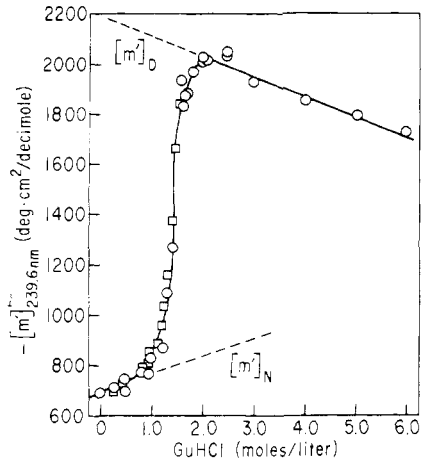

FIGURE 3: Optical rotation of RAFab at 239.6 nm as a function of Gdn·HCl concentration. (○) Forward solutions; (□) reverse solutions.

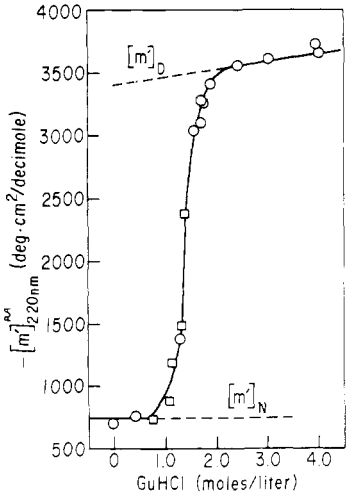

FIGURE 4: Optical rotation of RAFab at 220 nm as a function of Gdn·HCl concentration. (○) Forward solutions; (□) reverse solutions.

$$X_{\text{dissociation}} = \frac{\frac{1}{2}([m']_{L,N}+[m']_{Fd,N}-2[m']_N)}{[m']_D - [m']_N} = \frac{\Delta[m']_{\text{Dissociation}}}{\Delta[m']_{\text{total}}} = 0.35_{239.6\text{ nm}} \text{ and } 0.17_{220\text{ nm}}$$

$$X_{\text{L,denaturation}} = \frac{\frac{1}{2}([m']_{L,D} - [m']_{L,N})}{\Delta[m']_{\text{total}}} = \frac{\frac{1}{2}\Delta[m']_{\text{L,denaturation}}}{\Delta[m']_{\text{total}}} = 0.53_{239.6\text{ nm}} \text{ and } 0.40_{220\text{ nm}}$$

$$X_{\text{Fd,denaturation}} = \frac{\frac{1}{2}([m']_{Fd,D} - [m']_{Fd,N})}{\Delta[m']_{\text{total}}} = \frac{\frac{1}{2}\Delta[m']_{\text{Fd,denaturation}}}{\Delta[m']_{\text{total}}} = 0.12_{239.6\text{ nm}} \text{ and } 0.43_{220\text{ nm}}$$

The transition curves obtained for RAFab by $OR_{239.6}$, and OR_{220} are shown in Figures 3 and 4, respectively. The normalized data from these two curves are plotted in Figure 5 where

$$f_{\text{obsd}} = \frac{[m'] - [m']_N}{\Delta\,[m']_{\text{total}}}$$

In Figure 6 is shown the transition of SSFab as followed by $OR_{239.6}$ and the corresponding normalized curve is shown in Figure 7.

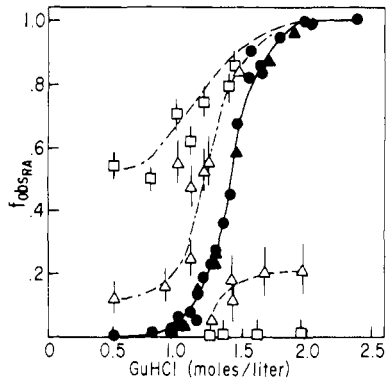

FIGURE 5: Normalized transition curve of RAFab. (●) data of Figure 3; (▲) data of Figure 4; (△) zero time points for slowest kinetic process; (□) zero time points for faster observed kinetic process.

Reversibility. The thermodynamic reversibility of the RAFab transition is demonstrated in Figures 3 and 4 by the agreement of forward solutions, made up by adding the Gdn·HCl last, and reverse solutions, made up by diluting preequilibrated solutions of protein in concentrated Gdn·HCl. In the center of the transition on the order of a week was required for the attainment of equilibrium.

In the case of SSFab, complete recovery of the native spectrum throughout the region shown in Figure 2 was obtained upon dilution of fully denatured SSFab to low Gdn·HCl concentration. However, as shown in Figure 6, in the transition region agreement between forward and reverse solutions was not attained after allowing 1 week for equilibration. Nevertheless, it was found that the forward and reverse solutions continued to approach each other over long periods of time as indicated on Figure 6; in addition all transition region solutions were capable of completely regaining the native state upon dilution to low Gdn·HCl concentration for periods up to 2 weeks. These observations, and some aspects of the kinetic results presented below, led to the conclusion that the transition of SSFab is thermodynamically reversible, but that the kinetics of equilibration are extremely slow under some conditions. The true equilibrium curve must lie between the curves defined by the most advanced forward and reverse points. The curve shown in Figure 7 represents the most advanced reverse points from Figure 6, considered for kinetic reasons to be the closest to equilibrium with respect to $OR_{239.6}$; this is the curve which will be considered in the further discussions.

Molecularity. The normalized transition curves for RAFab and SSFab measured at 239.6 nm are shown together in Figure 8 along with the L chain curve, also measured at 239.6 nm, from our previous report (Rowe and Tanford, 1973). It is seen that the midpoints of the RAFab and SSFab transitions are at 1.4 M Gdn·HCl and 1.6 M Gdn·HCl, respectively, while the isolated L chain has a transition midpoint at 1.15 M Gdn·HCl. It is clear from the relationships of these three curves that the L chains of RAFab and the L chain portion of SSFab are not free to denature in the Fab systems; i.e., the native material in the Fab transitions is predominantly associated. The finding that SSFab is more stable than RAFab is consistent with the conclusion that the noncovalent Fd–L interactions are maintained at concentrations of Gdn·HCl sufficient to denature the L chain; the greater stability of SSFab compared to RAFab is qualitatively explained by the enhancement of association in SSFab due to the disulfide bond. Therefore,

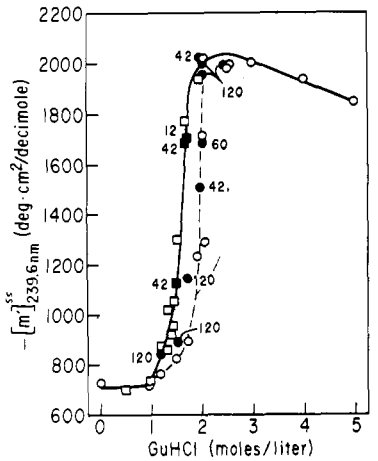

FIGURE 6: Optical rotation of SSFab at 239.6 nm as a function of Gdn·HCl concentration. (○) Forward solutions after waiting 8 days; (●) forward solutions after number of days indicated on graph; (□) reverse solutions after 8 days; (■) reverse solutions after number of days indicated.

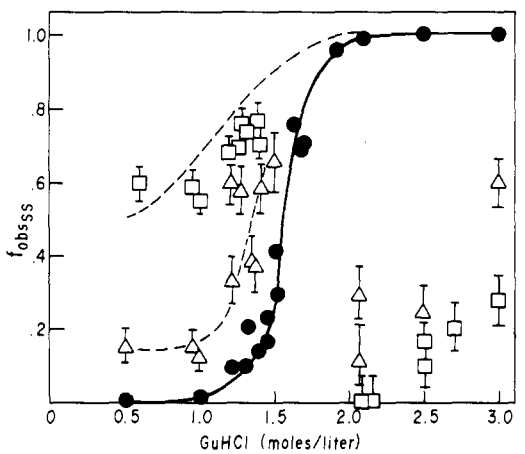

FIGURE 7: Normalized transition curve of SSFab. (●) "Equilibrium" data from Figure 6, chosen as described in test; (△) zero time points for slowest kinetic process; (□) zero time points for faster observed kinetic process.

while the transition of SSFab is unimolecular, the transition of RAFab is bimolecular.

Presence of Stable Intermediates. There are several established means of detecting stable intermediates in an equilibrium transition, that is, states other than the native and denatured states which are present in significant amounts under the conditions examined. One method is to compare the properties of the apparent equilibrium constant K_{ap} with those predicted for the true denaturation constant K_D. For example, using the procedure described by Tanford (1970) it is possible to approximately predict the dependence of the true denaturation equilibrium constant on denaturant concentration. This treatment yields the relation

$$\Delta G = -RT \ln K_D = \Delta G^\circ + \Delta\alpha \Sigma \delta g_{tr,i} \qquad (4)$$

where $\Delta\alpha$ is the average change in exposure to solvent of hydrophobic and peptide groups during unfolding and $\delta g_{tr,i}$ is the free energy of transfer of exposed group i from one solvent concentration to another. ΔG is the free energy of the transition in the solvent in question and ΔG° is the free energy of the transition in the absence of denaturant. $\Delta\alpha$ is 0.30–0.35 for the transition of globular proteins from N to D (Tanford, 1970) and $\delta g_{tr,i}$ for the appropriate groups in Gdn·HCl has been determined from solubility studies of model compounds (Nozaki and Tanford, 1970) so that the slope of a plot of ln K_D vs. Gdn·HCl concentration can be predicted if the amino acid composition is known. In the case of Wes Fab the predicted slope of such a plot is about 20.

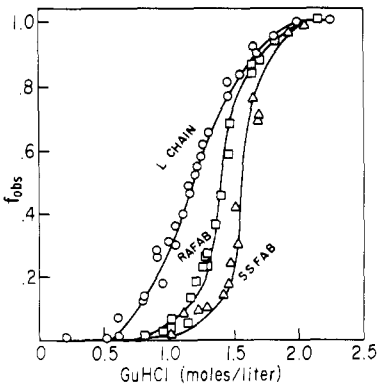

FIGURE 8: Normalized transition curves: (○) Wes L chain from Rowe and Tanford, (1973); (□) RAFab; (△) SSFab. All were obtained at 239.6 nm.

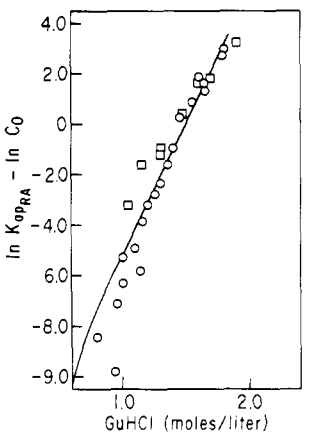

FIGURE 9: Dependence of apparent denaturation constant of RAFab on Gdn·HCl concentration. (○) Data of Figure 3; (□) data of Figure 4. Protein concentration c_0 is 3.6×10^{-6} mol/l.

In the case of the bimolecular denaturation of RAFab, the apparent equilibrium constant is

$$K_{ap,RA} = \frac{f^2_{obsd,RA} c_0}{1 - f_{obsd,RA}}$$

where c_0 is the molar concentration of Fab which is 3.6×10^{-6} M for the data of Figure 5. Figure 9 shows a plot of ln $K_{ap,RA}$ + constant vs. Gdn·HCl concentration. The slope of this plot is 10.4, approximately half the expected slope if $K_{ap} = K_D$, indicating that stable intermediates are present in this transition.

The apparent equilibrium constant for the unimolecular denaturation of SSFab is $K_{ap,SS} = f_{obsd,SS}/(1 - f_{obsd,SS})$. Figure 10 shows a plot of ln $K_{ap,SS}$ vs. Gdn·HCl concentration. The slope of this plot is 8.1, less than half the predicted slope if $K_{ap} = K_D$, indicating that the SSFab transition is even less cooperative than the RAFab transition, although it is significantly more cooperative than the L chain transition (Rowe and Tanford, 1973), in which a similar plot gave a slope of 4.8.

Consideration of the cooperativity of the denaturation transitions of RAFab and SSFab with respect to their de-

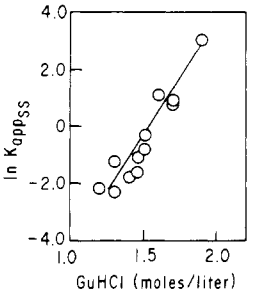

FIGURE 10: Dependence of apparent denaturation constant of SSFab on Gdn·HCl concentration.

pendence on Gdn·HCl concentration indicates that stable intermediates are present in both of these transitions. From the point of view of the denaturation models shown in Figure 1 it is of interest to consider whether free native L and Fd chains can account for the lowered cooperativity, or whether additional intermediates must be present, such as the half-denatured ones shown in Figure 1c and d. We have seen that Wes L chain is predominantly denatured throughout the Fab transitions (Figure 8). Figure 5 shows that the RAFab transition is the same whether measured by $OR_{239.6}$ or OR_{220}; since the denaturation of Fd piece contributes 43% of the Fab transition at 220 nm and only 12% of the transition at 239.6 nm the coincidence of the curves measured at these two wavelengths rules out a significant amount of free native Fd piece in the transition, leading to the conclusion that the apparent denaturation constant for Fd must be at least as large as that of L chain. These considerations suggest that intermediates other than free native Fd or L chains are present in the transitions.

The most compelling evidence that stable intermediates other than free native chains are present is the observation that the SSFab transition is no more cooperative than the RAFab transition, indicating that stable intermediates are at least as important in the SSFab transition as they are in the RAFab transition. Independent of the absolute values of $K_{ap,L}$ and $K_{ap,Fd}$, it is clear that free chains would be less native in the SSFab transition than in the RAFab transition, because the SSFab transition occurs at higher Gdn·HCl concentration. In contrast, one would expect that any associated intermediates, such as those shown in Figure 1c and d, would be stabilized by the disulfide bond of SSFab, and could be more important in SSFab denaturation even though it occurs at higher denaturant concentration.

Kinetics of the Approach to Equilibrium. The presence of stable intermediates in an equilibrium transition can be unequivocally established by following the kinetics of the approach to equilibrium (Tanford, 1968, 1970); if stable intermediates are present, as already demonstrated for RAFab and SSFab, kinetic studies provide information concerning the identity of intermediates and the mechanism of folding and unfolding. If a unimolecular process is two-state, i.e., $N \rightleftharpoons D$, then solution of the appropriate rate equations gives the result

$$\left|\frac{\alpha_\infty - \alpha_t}{\alpha_\infty - \alpha_0}\right| = e^{-(k_f+k_r)t} \qquad (5)$$

where α is the optical rotation at the subscripted time. If intermediates are present at equilibrium, solution of the rate equations take the form

$$\left|\frac{\alpha_\infty - \alpha_t}{\alpha_\infty - \alpha_0}\right| = \sum_i p_i e^{-\lambda_i t} \qquad (6)$$

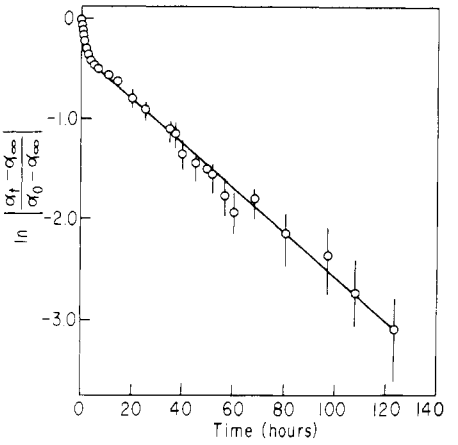

FIGURE 11: Kinetics of unfolding of RAFab in 1.6 M Gdn·HCl followed by optical rotation at 239.6 nm.

where the λ's are functions of the rate constants and the p's are functions of both the rate constants and the physical properties of the intermediates with respect to the observed property. The exact solution depends on the mechanism, but all reversible first-order mechanisms give solutions of this form.

A survey of the kinetics of the approach to equilibrium of RAFab and SSFab was performed by following the optical rotation at 239.6 nm as a function of time. The purpose of these experiments was to examine the general characteristics of the kinetics in terms of the unusually slow rates, the presence of intermediates, and as a means of comparing RAFab and SSFab. The data were treated as first order by plotting ln $[(\alpha_\infty - \alpha_t)/(\alpha_\infty - \alpha_0)]$ vs. time, even though some of the RAFab processes must be second order. In all experiments nonlinear plots were obtained; however, they could be adequately described by eq 6 and could be resolved into two or three apparently first-order terms. Figures 11 and 12 show examples of the unfolding and refolding kinetics, respectively, of RAFab, and Figure 13 shows an example of the refolding kinetics of SSFab.

In the case of RAFab, kinetic measurements were made throughout the transition region. In the forward experiments (Figure 11), the observed data extrapolate to zero at zero time, and are completely described by two terms in eq 6. In contrast, although in most cases the reverse experiments could be described by two first-order terms (e.g., Figure 12), the faster process did not extrapolate to zero at zero time, making a total of three terms of eq 6 necessary to describe the data. This result indicates the presence of at least two stable intermediates in the transition region. Under conditions where both forward and reverse experiments could be performed (near the center of the transition) the apparent rate constants for the slowest process were the same, confirming the reversibility of the mechanism. The extrapolated zero time points for the linear portions of the kinetic plots are shown in Figure 5 for RAFab. The points below the transition region suggest that the fastest process contributes about 0.5 to the total change in $OR_{239.6}$, the second contributes 0.35, and the slowest about 0.15.

In the case of SSFab, the extremely slow rates of equilibration in the transition region precluded kinetic measurements under some conditions. However, as illustrated by comparison of Figures 12 and 13, the general appearance of the SSFab kinetics was similar to that of the RAFab data

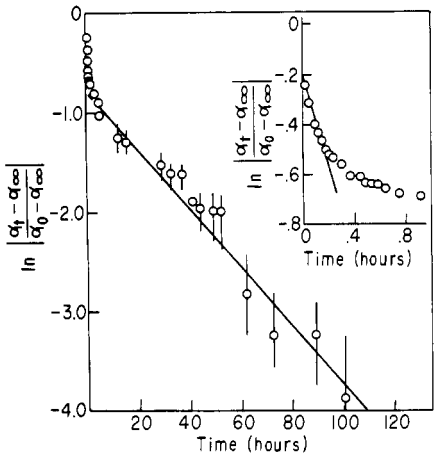

FIGURE 12: Kinetics of refolding of RAFab in 1.2 M Gdn·HCl, followed by optical rotation at 239.6 nm. Inset represents first hour.

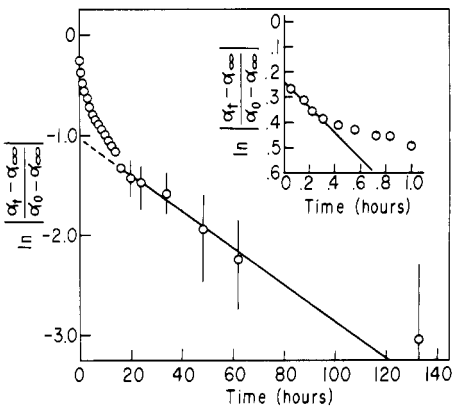

FIGURE 13: Kinetics of refolding of SSFab at 1.4 M Gdn·HCl, followed by optical rotation at 239.6 nm. Inset represents the first hour.

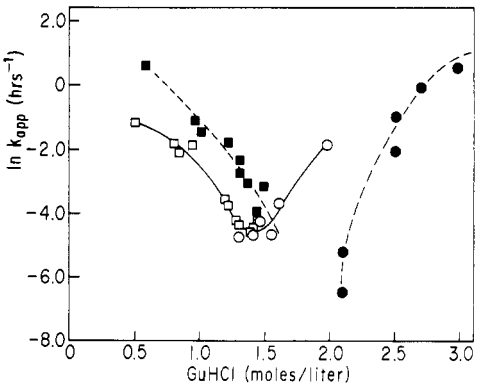

FIGURE 14: Apparent rate constants for slowest processes of RAFab and SSFab. (○) RAFab unfolding; (□) RAFab refolding; (●) SSFab unfolding; (■) SSFab refolding.

under conditions where both could be measured. This similarity is most apparent in the extrapolated zero time points of the linear portions of the kinetic data for experiments below the transition regions, shown in Figure 7 for SSFab and in Figure 5 for RAFab. This similarity suggests that the identity of intermediates appearing in the two systems is the same, although the rate constants governing their appearance are different.

The most remarkable aspect of the kinetics of equilibration of RAFab and SSFab is the unusually slow rates observed for these reversible processes in the transition regions. Although equilibration above and below the transition regions was rapid in both systems, as shown in Figure 14, the apparent rate for the slowest step for RAFab goes through a minimum of 0.008 h^{-1} in the center of its transition, and the rates for SSFab equilibration are probably considerably smaller than this in the center of its transition.

Although a quantitative kinetic analysis was not attempted, some general conclusions regarding the origin of these slow rates may be reached by comparison of these rates with those obtained for isolated L chain (Rowe and Tanford, 1973). The unfolding of RAFab in the transition region (e.g., Figure 11) is completely described by two apparent rate constants; both of these rate constants are several orders of magnitude smaller than the slowest rate observed in the denaturation of the isolated L chain. It must be concluded therefore that the unfolding of the L chain half of RAFab is preceded by a rate-limitng process involving its interaction with the Fd portion of the molecule. Moreover, the finding of two such processes indicates that the dissociation process involves two steps, with a half-dissociated form as an intermediate. In the renaturation kinetics, the two slow processes are preceded by a process too fast to be quantitated by our technique; since the total contribution of this process is approximately 0.5 it is likely that this process represents the preequilibration of the individual chains prior to association.

The conclusion that the unusually slow rates observed in these systems are due to the association–dissociation reaction between the Fd and L chains is supported by the relationship between the apparent rate constants for RAFab and SSFab. In Figure 14 the apparent rate constants for the slowest process in each experiment are shown for RAFab and SSFab; as shown here, at a given Gdn·HCl concentration refolding of SSFab is faster than RAFab (i.e, at low Gdn·HCl concentration) and unfolding is slower (i.e., at high Gdn·HCl concentration). It is to be expected that the interchain disulfide bond would enhance the association between chains, increasing the rate of renaturation and decreasing the rate of denaturation of SSFab relative to RAFab.

Thermodynamic Properties of the Domain Structure. We have shown that the denaturation data for RAFab and SSFab are independently consistent with the domain denaturation models illustrated in Figure 1c and d; because the monomeric domains are predominantly unfolded in the Gdn·HCl concentrations at which the Fab transitions occur, one can neglect the small amounts of species which have one or more native monomeric domains. In these models the overall denaturation equilibrium constant for RAFab is given by

$$K_{D,RA} = K_{1R}K_{2R} = K_{3R}K_{4R} = \frac{4f_{DL}f_{DFd}\,c_0}{f_{N,RA}}$$

and for SSFab

$$K_{D,SS} = K_1K_2 = K_3K_4 = f_D/f_N$$

Each microscopic region denaturation constant can be represented as the product of two monomeric domain denaturation constants and a dissociation constant or a pseudodissociation constant, as represented in eq 2 or 3. For example, the process designated by K_{1R} is analogous to that shown in Figure 1b, and $K_{1R} = K_{d,1R}K_{VL}K_{VF}$ where K_{VL} and K_{VF} are the denaturation constants for monomeric v_L and v_H domains, respectively. Similarly, the process designated by K_{4R} is analogous to that of Figure 1a, and K_{4R} =

$K_{d,4R}K_{VL}K_{VF}$. The overall denaturation constants can be expressed as

$$K_{D,RA} = K_{d,1R}K_{d,2R}K_{VL}K_{VF}K_{CL}K_{CF} = K_{d,3R}K_{d,4R}K_{VL}K_{VF}K_{CL}K_{CF}$$

where $K_{d,2R}$ and $K_{d,4R}$ are bimolecular dissociation constants, and $K_{d,1R}$ and $K_{d,3R}$ are unimolecular pseudodissociation constants. For SSFab we have $K_{D,SS} = K_{d,1}K_{d,2}K_{VL}K_{VF}K_{CL}K_{CF} = K_{d,3}K_{d,4}K_{VL}K_{VF}K_{CL}K_{CF}$ where all the equilibrium constants are unimolecular.

There are eight microscopic region denaturation constants indicated in Figure 1c and d, four for each dimeric region of Fab; the differences among the equilibrium constants for either region are in the dissociation or pseudodissociation constants. Although sufficient information does not exist to solve for all eight of the region denaturation constants indicated in Figure 1c and d, by taking advantage of the known relationships among those for each region, some important relationships between the two regions can be deduced by interpreting the data in terms of these models.

The most important conclusion about the structure of the Fab fragment which can be made by an interpretation of all the data in terms of this model is that one of the two dimeric regions of Fab is intrinsically more stable than the other. This conclusion is based on the unequivocal demonstration that at least one of the half-denatured intermediates illustrated in Figure 1c is present in the denaturation transition of RAFab. As indicated in the illustration there are two denaturation constants in RAFab for each region, one unimolecular (e.g., K_{1R} for the V region), represented by an equation of the form of eq 3, and one bimolecular (e.g., K_{4R}), represented by an expression of the form of eq 2. At the protein concentrations used in this study it may be assumed that the *extent* of the reaction governed by the bimolecular constant (e.g., K_{4R}) must be orders of magnitude greater than the extent of the *same* reaction governed by a unimolecular constant (e.g., K_{1R}). If the unimolecular constants K_{1R} and K_{3R} were similar in magnitude, because the extent of the reactions they govern would be orders of magnitude less than the extent of the corresponding bimolecular reactions governed by K_{4R} and K_{2R}, respectively, then neither intermediate P1R or P2R could be stable. Since we have found that one of these intermediates is stable, then K_{1R} and K_{3R} cannot be similar in magnitude. Since K_{1R} and K_{3R} are both unimolecular, they can be directly compared; the difference between them is a measure of the intrinsic difference in stability between the C and V regions of Fab.

The SSFab data are consistent with the conclusion that one of the regions of Fab is intrinsically more stable than the other and permit a maximum limit to be placed on the ratio K_1/K_3 (we assume that K_1 and K_3 are similar to K_{1R} and K_{3R}, respectively). As illustrated in Figure 1d, all the equilibrium constants in SSFab are unimolecular and can be represented by expressions of the form of eq 3. This means that if $K_3 \ll K_1$, then $K_2 \ll K_1$ also, and the intermediate P1 would be more stable than the corresponding RAFab intermediate P1R; this is consistent with the finding that the RAFab transition is at least as cooperative as the SSFab transition. In fact, it can be shown that if $K_2 < 0.01K_1$ separate stages would be observed in the SSFab transition. Thus, while it is reasonable that K_2 may be slightly larger than K_3, the lack of separate stages in the SSFab transition suggests that the ratio of K_1 to K_3 is not greater than three orders of magnitude. The conclusion that the ratio of K_1 and K_3 is from two to four orders of magnitude was also obtained in a computer simulation study using the complete model (i.e., including species not included in Figure 1c and d in which one or more of the dissociated domains are folded), in which the relative positions of the two curves was also taken into account (Rowe, 1971).

Our data are not sufficient alone to identify whether the C or V region is the more stable (i.e., $K_1/K_3 \ll 1$ or $\gg 1$); however, the x-ray crystallographic results of Poljak et al. (1973) show that for the human myeloma Fab fragment New, the C region is more compact than the V region, and that the two domains of the C region are more closely associated than those of the V region. These data and some other lines of evidence discussed below suggest that it is the C region of Wes Fab which is the more stable.

Fd–L Interactions. The results of this study show that the interactions between the heavy and light chain portions of Fab are extremely strong, and are maintained at Gdn·HCl concentrations sufficient to denature the isolated domains. Numerical values for the microscopic dissociation and pseudodissociation equilibrium constants could be determined from equations of the form of eq 2 and 3 if all the denaturation constants were known. The region denaturation equilibrium constants for RAFab may be estimated by assuming that at the center of the RAFab transition $f_{N,R} = f_{P1R} = f_{DL} + f_{DF}$. This leads to $K_{1R} = 1$, $K_{2R} = 10^{-6}$ M, and $K_{D,RA} = 10^{-6}$ M. If we let $K_{3R} = 0.001$, we have $K_{4R} = 10^{-3}$ M, since $K_{1R}K_{2R} = K_{3R}K_{4R}$. Maximum order of magnitude estimates of the microscopic dissociation and pseudodissociation constants at the center of the RAFab transition (1.4 M Gdn·HCl) can then be made, using eq 2 or 3 by letting K_{VF} and K_{CF} take their minimum values equal to $K_{VL} = K_{CL} = K_{ap,L}$ determined experimentally (Rowe and Tanford, 1973). This calculation gives for the less stable V region a unimolecular dissociation constant $K_{d,1R} = 0.1$ and a bimolecular dissociation constant $K_{d,4R} = 10^{-4}$ M. For the more stable C region the unimolecular dissociation constant is then $K_{d,3R} = 10^{-4}$ and the bimolecular constant is $K_{d,2R} = 10^{-7}$ M. If the Fd domains are less stable than the L domains, the dissociation constants would be smaller than these estimates.

These estimates of the dissociation constants between the domains of the Fd and L chains demonstrate some important aspects of the Fd–L interaction. It is seen that the more stable C region is primarily responsible for maintaining the association, having a bimolecular constant of 10^{-7} M even in 1.4 M Gdn·HCl. In a bimolecular sense, the interaction between the V domains is relatively weak, and may not be sufficient to maintain the associated state at ordinary protein concentrations; however their covalent connections to the strongly associated C region, leading to unimolecular association, give rise to a pseudodissociation constant of 0.1, enabling the V region to exist predominantly in the associated state independent of protein concentration. The biological importance of this feature of the Fab structure will be discussed below.

Intrinsic Properties of Fab. The thermodynamic properties of a protein under physiologic conditions can be obtained by extrapolating the equilibrium constants determined as a function of denaturant concentration to zero denaturant concentration, using a function such as that given by eq 4. The denaturation equilibrium constants extrapolated to zero Gdn·HCl concentration give a measure of the intrinsic stability of the native structure over the randomly

coiled cross-linked polypeptide chains. The extrapolated dissociation constants give a measure of the contribution of the interchain interactions to the stability of the native structure.

The estimates of the several equilibrium constants obtained in the present study of Fab are not sufficiently accurate as a function of Gdn·HCl concentration for a direct extrapolation to zero Gdn·HCl concentration; however, we have

$$\Delta G^\circ_{\text{region}} = \Delta G^\circ_{\text{L domain}} + \Delta G^\circ_{\text{Fd domain}} + \Delta G^\circ_{\text{dissociation}}$$

From the independent study of Wes L chain we have $\Delta G^\circ_{\text{L domain}} = 5.5$ kcal/mol. A minimum estimate of the intrinsic stability of each region of Fab may be made by assuming that the Fd domains have their maximum stability equal to that of the L domains, and that the unimolecular and bimolecular dissociation constants are the same in the absence of Gdn·HCl as they were estimated to be in 1.4 M Gdn·HCl. The alternate assumption, that the Fd domains were less stable than the L domains, would lead to the same $\Delta G^\circ_{\text{region}}$ as before, but with a greater contribution from the domain–domain interactions. The assumption that some of the dependence on Gdn·HCl of the $\Delta G^\circ_{\text{region}}$ was contained in the dissociation portion of the free energy would lead to a greater intrinsic stability of the region and a greater contribution from the interdomain interactions. While the assumptions chosen are not necessarily the most realistic among these possibilities, they were chosen to provide the minimum estimate of effects which are quite important even at a minimum.

These calculations lead to an estimate of $\Delta G^\circ_{\text{C region}} = 15$ kcal/mol, with 4 kcal/mol being contributed by the domain–domain interaction. For the less stable V region we obtain $\Delta G^\circ_{\text{V region}} = 12$ kcal/mol, with 1.3 kcal coming from the interdomain interaction. These again show the importance of the interdomain interaction in the constant region; this interaction contributes at a minimum almost one-third of the total stability of this region, suggesting that a large contact area involving many amino acid residues is involved. In contrast, the contribution of the interaction between the V domains is relatively less, and probably involves a smaller contact area.

Discussion

The results of our study are consistent with the domain structure of Fab. Our results demonstrate the importance of the pairwise interactions between the domains of opposing chains in the native Fab fragment, and suggest that rather than considering it in terms of four independent domains it is functionally more realistic to consider the Fab portion of antibodies as being composed of two independently folded and associated regions. This concept of the Fab fragment is supported by the x-ray crystallographic results of Poljak et al. (1973) on Fab New. Our denaturation equilibrium results indicate further that in spite of the structural homologies between the two dimeric regions of the Fab fragment, these two regions are considerably different thermodynamically. This difference is manifested as a several order of magnitude difference in stability toward Gdn·HCl denaturation which can be attributed largely to a difference in the mode and free energy of the noncovalent interdomain interactions in the two regions. In the more stable region the interdomain interaction contributes a minimum of nearly one-third of the free energy of stabilization of this region in the absence of denaturant, indicating an extensive contact area between these two domains. This large contact area suggests that it is this region in which the known conformational change occurs upon dissociation, such that some of the exposed contact residues are reshielded from solvent. In contrast, in the less stable region the minimum estimate of the free energy contribution of the interdomain interaction is less than 2 kcal/mol, suggesting a limited contact area involving a relatively small portion of the sequences of each domain. We have identified the more stable primary interaction region as the constant region on the basis of our results combined with some literature reports. (1) We have suggested that the more stable region is the one in which a conformational change occurs upon dissociation. Painter et al. (1972) showed that no conformational change occurs in the binding site region of rabbit anti-Dnp antibodies upon dissociation. (2) It is now well established that H and L chains can recombine in vitro with partners other than their original ones to form molecules which are structurally indistinguishable from naturally occurring immunoglobulins (e.g., Björk and Tanford, 1971c; Painter et al., 1972). (3) This conclusion is not inconsistent with data indicating variability in H–L interactions, since we have seen that the V region does contribute to the H–L interaction even if it is not the primary interaction site. (4) X-ray crystallographic data on a human Fab fragment (Poljak et al., 1973) and on a mouse myeloma Fab fragment (Padlan et al., 1973) show that the C region is more compact than the V region in both of these proteins, and that the C domains interact over a wider area than the V domains.

Consideration of the x-ray crystallographic structure of Fab determined by Poljak et al. (1973) provides an explanation of our thermodynamic findings. The structure shows that each of the four homology regions has similar folding; they contain two regions of β-pleated sheet, one consisting of three stretches of amino acid chain, and one consisting of four stretches of chain. Examination of the structure of the whole Fab fragment, however, leads to the remarkable observation that the v_L–v_H contacts involve residues from the three-chain sheets, whereas the c_L–c_H contacts involve residues from the four-chain sheets. Thus, in spite of the structural homologies in the four domains, the interdomain interactions in the two dimeric regions of Fab are not homologous in either structure or regions of sequence! This observation explains our finding that the C and V regions of Fab are very different in thermodynamic properties in spite of the structural homologies of the individual domains.

Our study of the dissociation and denaturation of the Fab fragment reveals some important thermodynamic features of its unique tertiary quaternary structure in which four independently folded domains are connected pairwise in one dimension by covalent linkages and pairwise in another dimension by noncovalent interactions. For example, at the level of the dimeric regions, the advantage in stability gained by the noncovalent association of independently folded globular protein moieties is demonstrated, and is probably a common phenomenon in protein structure, considering the large number of multisubunit proteins which is known. At the level of the whole two region Fab fragment an overall gain in stability results from the covalent linkage between the domains of either chain (e.g., v_L–c_L, etc.), due to the effect of these connections on the association of the chains. For example, in spite of its weakness in the classical bimolecular sense, the V region interaction contributes significantly to the association of the chains when its associa-

tion is made unimolecular by its connection to the associated C region. This effect explains reports that neither the isolated v_L or c_L domains bind to H chain as well as the intact L chain (Smith and Dorrington, 1972; Karlsson, 1972). The effect of v_L–c_L and v_H–c_H linkages is even better appreciated when considered from the point of view of the V region: the covalent attachment of the V domains to the strongly associated C region enables them to remain predominantly in the associated state, independent of protein concentration, in spite of their weak intrinsic attractions for each other as measured in a bimolecular sense.

The results obtained in the present study pertain to the Fab fragment from an individual homogeneous human IgG myeloma protein. However, the applicability of our interpretation to IgG in general is indicated by consideration of several kinds of data on other proteins. For example, extremely slow kinetics of equilibration or unfolding in Gdn·HCl have been observed for the Fab from another myeloma protein (E. S. Rowe, unpublished results), and for rabbit antibody Fab fragments (Whitney, 1964; Cathou and Haber, 1967; Cathou and Werner, 1970). The relationships between the isolated chains and the associated states which we have documented for Wes Fab are consistent with a report of the unfolding in Gdn·HCl of several whole IgGs and their isolated chains in which it was found that the extent of unfolding after 12 h in Gdn·HCl was greater for the isolated chains than for the wholg IgG (Lapanje and Dorrington, 1973). Since this is not equilibrium data, no conclusions concerning the relative stabilities can be drawn; however, qualitatively these results are consistent with our finding that the kinetics of equilibration of the associated states are much slower than those of the isolated chains. Our conclusion that the Fd–L interaction occurs primarily through the constant domains (c_L and c_{H1}) is consistent with gel electrophoresis results showing that the release of L chains under denaturing conditions is dependent on the class and type, i.e., on the constant portions, of the immunoglobulin chains (Zimmerman and Grey, 1972; Cohen and Gordon, 1965). All of these data are consistent with the interpretation which we have derived from our study of an individual Fab fragment and indicate that it is a typical representative. Based on our results, other individual $IgG_1\kappa$ Fab fragments are expected to have similar but not identical stabilities due to V region differences, whereas Fab fragments of other types and classes probably have greater differences in stability due to the differences in the C regions as well. These differences reflect variations in both the interdomain interactions and the intrinsic domain stabilities. However, the extremely slow kinetics of unfolding in Gdn·HCl which are observed for heterogeneous IgG Fab from both rabbit (Whitney 1964) and human IgG, which we have related to the strong Fd–L interaction, suggest that the general relationships between the domain stabilities and the interdomain interactions which we have derived for Wes Fab may be widely applicable.

Kinetics of the Approach to Equilibrium. One of the objects of the present investigation was to elucidate the apparently remarkable behavior of the Fab fragment in the presence of Gdn·HCl in terms of the slow conformational changes which had been observed. Although the complexity of the model required to describe the equilibrium states of the Fab fragment precluded a quantitative analysis of the kinetic mechanism involved in the approach to equilibrium, we have shown that the rate-limiting steps for these slow reversible processes involve the association–dissociation reaction. One possibility is that the association and dissociation are themselves extremely slow under some conditions; however, our finding that complete refolding is quite rapid at concentrations of Gdn·HCl below the transition region suggests that association is reasonably rapid at pH 7, as was also indicated in a recent study of H–L recombination at pH 5 (Bigelow et al., 1974). The more plausible alternative possibility, suggested by our estimates of the dissociation and denaturation equilibrium constants at intermediate Gdn·HCl concentrations, is that the slow rates of overall equilibration are a consequence of the simultaneous conditions that the dissociation (or pseudodissociation) equilibrium constants are small but finite while the separated or dissociated subunits are not thermodynamically stable. Equilibration could then occur slowly through the small steady-state concentration of free folded domains, even if the individual rate constants for dissociation, association, unfolding, and refolding are relatively large.

This explanation of the slow equilibration of the Fab fragment in Gdn·HCl solutions may represent a rather common phenomenon. The literature of enzymology is full of multichain "labile" enzymes which lose activity upon storage over periods of time ranging from days to weeks or even months. This observation may indicate that these enzymes are in a situation, similar to that of Fab fragment in Gdn·HCl, where the equilibrium constants for dissociation of subunits are small but finite while the free subunits are not stable, so that in dilute solutions unfolding occurs through small amounts of dissociated subunits. This consideration has important implications because it suggests that some biologically active proteins are not thermodynamically stable under physiologic solvent conditions, even though they have relatively long lifetimes in vivo.

Biological Considerations. The biological importance of the noncovalent Fd–L interactions is indicated by the fact that both chains contribute to antibody specificity. As discussed above, the evidence is accumulating that the Fd–L interaction is nonspecific with respect to the association of particular H and L chain sequences; this nonspecificity is consistent with the suggestion of Edelman and Gally (1964) that the chains are independently variable in vivo giving rise to a potential diversity of specificities which far exceeds the number of sequences available for each chain. On the other hand, comparison of the properties of the Fd–L interaction with the self-associating properties of Fd and L chains shows that the Fd–L interaction is highly specific in the sense that it is different than and much stronger than the self-attractions of L chains and Fd chains. Studies on isolated Fd (Huston et al., 1972) and L chains (Berggard and Peterson, 1969; Bernier and Putnam, 1964; Björk and Tanford, 1971a; Gally and Edelman, 1964; Green, 1973; Rowe and Tanford, 1973) show that their self-attractions are extremely variable, generally weak, and usually involve no conformational changes. For example heterogeneous mixtures of L or Fd chains contain both monomers and dimers, with a wide range of association constants, whereas homogeneous L chains may be either monomeric or dimeric at ordinary protein concentrations. These results suggest that the self-associations occur through the V domains while the C domains have little self-attraction. An apparent exception is the disulfide linked L dimer Mcg which has been analyzed by x-ray diffraction (Schiffer et al., 1973) in which the c_L–c_L interaction appears to mimic the c_L–c_{H1} interaction of Fab (Poljak et al., 1973); however, no thermodynamics have been done on this system, and our model shows

that the presence of a disulfide link and the association of a neighboring region (in this case the v_L region) can cause the association of two domains which have relatively weak intrinsic attractions. In contrast, the Fd-L interaction is strong, involves a conformational change, and, except in the case of disulfide linked L dimers, is always preferred over the self-associations. These considerations indicate that the Fd and L chains are specifically complementary at the primary interaction site. This specificity ensures that each antigen binding site is composed of unlike chains, which in turn leads to the tetrameric whole IgG structure through the association of the Fc portions of the H chains. This specificity is biologically essential, since the bivalent tetrameric structure is required for the full physiological activity of IgG.

We have seen that the Fab region of IgG is composed of two independently folded and associated regions, raising the question of the biological importance of this remarkable tertiary-quaternary strucutre. A possible answer to this question may lie in our finding that the C region functions as the site of the specific Fd-L interaction and provides most of the free energy needed to complete the assembly of the V region antigen binding site by making the association of the V domains unimolecular. Implicit in the generation of antibody diversity by sequence variability there are several restrictions on the sequences of the v_L and v_H domains which can be successful in producing a functional antibody. First, the sequences generated must be capable of folding into a specific globular conformation; evidently, the invariant residues of the V domains reflect this requirement. Secondly, a potential partial binding site for some antigenic determinant must be formed. The third requirement, resulting from the fact that both chains contribute to antigen binding, is that the variable domains of each chain must be capable of interacting with the V domain of an opposing chain in such a way that the partial antigen binding sites are juxtaposed. Finally, if the chains are independently variable, then each v_L domain must be capable of interacting with a variety of v_H domains, while at the same time it must not associate with another v_L domain, and similarly for the v_H domains. The first two restrictions are similar to those involved in the evolution of any globular protein having a specific function; since globular proteins are only marginally stable, it has been suggested that amino acid sequences satisfying these two criteria are relatively improbable. From this point of view it would seem that the last two restrictions on v_L and v_H variability would present an almost insurmountable difficulty if the C domains were not present. The covalent attachment of the v_L and v_H domains to the c_L and c_H domains, respectively, reduces the last two restrictions to the requirement that the V domains must have a minimum capability of interacting with a variety of other V domains in such a way that their partial binding sites are juxtaposed. As we have shown, by making the association of the V domains unimolecular, the C region enables the V domains to exist in the associated state even if their attractions are very weak; in addition, the V domains need not discriminate between v_L and v_H partners (as the self-associating properties of Fd and L chains suggest they do not) if the C domains are specifically complementary. Thus the presence of the C region enhances the potential V domain variability by greatly reducing the requirement for v_L-v_H association both in affinity and specificity. The corresponding gain in potential antibody diversity would appear to be sufficient to account for the selective pressure which led to the remarkable tertiary-quaternary structure of the Fab portion of antibodies.

References

Berggard, I., and Peterson, P. A. (1969), *J. Biol. Chem. 244, 4299.*

Bernier, G. M., and Putnam, F. W. (1964), *Biochim. Biophys. Acta 86,* 295.

Bigelow, C. C., Smith, B. R., and Dorrington, K. J. (1974), *Biochemistry 13,* 4602.

Björk, I., and Tanford, C. (1971a), *Biochemistry 10,* 1271.

Björk, I., and Tanford, C. (1971b), *Biochemistry 10,* 1280.

Björk, I., and Tanford, C. (1971c), *Biochemistry 10,* 1289.

Cathou, R. E., and Haber, E. (1967), *Biochemistry 6,* 513.

Cathou, R. E., and Werner, T. C. (1970), *Biochemistry 9,* 3149.

Cohen, S., and Gordon, S. (1965) *Biochem. J. 97,* 460.

Dorrington, K. J., and Kortan, C., (1974), *Biochem. Biophys. Res. Commun. 56,* 529.

Dorrington, K. J., and Smith, B. R. (1972), *Biochim. Biophys. Acta 263,* 70.

Dorrington, K. J., and Tanford, C. (1970), *Adv. Immunol. 12,* 333.

Edelman, G. M., and Gally, J. A. (1964), *Proc. Natl. Acad. Sci. U.S.A. 51,* 864.

Edelman, G. M., Gall, W. E., Waxdal, M. J., and Konigsberg, W. H. (1968), *Biochemistry 7,* 1950.

Fish, W. F., Mann, K. G., and Tanford, C. (1969), *J. Biol. Chem. 244, 4989.*

Fleischman, J. B., Pain, R. H., and Porter, R. R. (1963), *Arch. Biochem. Biophys., Suppl. 1,* 174.

Gally, J. A., and Edelman, G. M. (1964), *J. Exp. Med. 119,* 817.

Green, R. W. (1973), *Biochemistry 12,* 3225.

Huston, J. S., Björk, I., and Tanford, C. (1972), *Biochemistry 11,* 4256.

Karlsson, F. A. (1972), *J. Immunol. 109,* 110.

Keilly, W., and Harrington, W. F. (1960), *Biochim. Biophys. Acta 41,* 401.

Lapanje, S., and Dorrington, K. J. (1973), *Biochim. Biophys. Acta 322,* 45.

Lebovitz, H. E., Delany, R., Fellows, R. E., Jr., and Hill, R. L. (1968), *J. Biol. Chem. 243,* 4197.

Mannik, M. (1967), *Biochemistry 6,* 134.

Nozaki, Y., and Tanford, C. (1970), *J. Biol. Chem. 245,* 1648.

Padlan, E. A., Segal, D. M., Spade, T. F., Davies, D. R., Rudikoff, S., and Potter, M. (1973), *Nature (London), New Biol. 245,* 165.

Painter, R. G., Sage, H. J., and Tanford, C. (1972), *Biochemistry 11,* 1327, 1338.

Poljak, R. J., Amzel, L. M., Avey, H. P., Chen, B. L., Phizackerley, R. P., and Saul, F. (1973), *Proc. Natl. Acad. Sci. U.S.A. 70, 3305.*

Porter, R. R. (1959), *Biochem. J. 73,* 119.

Rowe, E. S. (1971), Ph.D. Thesis, Duke University, Durham, N.C.

Rowe, E. S., and Tanford, C. (1972), *Fed. Proc., Fed. Am. Soc. Exp. Biol. 31,* 750.

Rowe, E. S., and Tanford, C. (1973), *Biochemistry, 12,* 4822.

Schiffer, M., Girling, R. L., Ely, K. R., and Edmundson, A. B. (1973), *Biochemistry 12,* 4620.

Smith, B. R., and Dorrington, K. J. (1972), *Biochem. Bio-*

phys. Res. Commun. 46, 1061.
Stevenson, G. T., and Dorrington, K. J. (1970), *Biochem. J. 118,* 703.
Tanford, C., (1968), *Adv. Protein Chem. 23,* 121.
Tanford, C. (1970), *Adv. Protein Chem. 24,* 1.
Whitney, P. L. (1964), Ph.D. Thesis, Duke University, Durham, N.C.
Wilson, W. D., and Foster, J. F. (1970), *Biochem. Biophys. Res. Commun. 38,* 552.
World Health Organization (1964), *Bull. W.H.O. 30,* 447.
Zimmerman, B., and Grey, H. M. (1972), *Biochemistry 11,* 78.

Estrogen Receptors in the Rat Uterus. Retention of Hormone–Receptor Complexes†

Joe V. Juliano and George M. Stancel*

ABSTRACT: The retention pattern and biochemical characteristics of estrogen receptors in the nuclei of uterine cells were studied as a function of time after the in vivo injection of estradiol (E_2) to immature female rats. One hour after the injection of 0.1 μg of tritiated E_2, approximately 0.20 pmol per uterus of receptor bound hormone is retained in uterine nuclei. This dose of E_2 produces a maximal uterotrophic response. Six hours after E_2 administration, uterine nuclei retain 0.04–0.08 pmol of hormone per uterus. Hormone receptor complexes extracted from uterine nuclei 1, 3, and 6 h after in vivo injection of hormone have similar structural and binding characteristics. Receptors extracted at all three times sediment at 5S in high salt gradients and have a dissociation binding constant of approximately 3 nM for E_2. The wash-out curves of receptors as a function of salt concentration are identical for uterine nuclei from animals treated for 1 or 6 h with estradiol, suggesting that the nature of the nuclear binding of receptors is not altered during this time interval. Experiments utilizing the injection of unlabeled estradiol, followed by an in vitro exchange procedure with tritiated estradiol, indicated that the total nuclear estrogen receptor sites, i.e., filled and vacant, decreased similarly.

The initial event in the action of a steroid hormone with a target tissue is thought to be the formation of a complex between the hormone and a specific cytoplasmic receptor protein. Following hormone-receptor interaction in the cytoplasm, the complex appears to migrate to the nucleus of the target cell, where it is bound to nuclear components, or nuclear acceptor sites. This nuclear localization of the receptor–hormone complex is thought to stimulate transcription, and thus initiate a sequence of biochemical events which ultimately culminate in the overall physiological changes produced by the hormone (Gorski, 1973; Williams, 1974; Jensen and DeSombre, 1973). A number of different steroid hormones studied to date appear to exert their effects via this general type of "cascade" mechanism (Jensen and DeSombre, 1972; O'Malley et al., 1971).

One system which has been extensively studied is the stimulation of the immature rat uterus by estrogens. Numerous studies with this system have focused on the characterization of estrogen receptors (Puca et al., 1972; Stancel et al., 1973a,b; Jensen et al., 1971), the nuclear localization of estrogen receptors (Shymala and Gorski, 1969; Jensen et al., 1968; Puca et al., 1974), and the effects of estrogen treatment on uterine RNA synthesis (O'Malley and Means, 1974; Hamilton, 1971; Glasser et al., 1972; Gorski, 1964). In this communication we present the results of studies on the nuclear retention patterns of estrogen receptors in uterine nuclei and characteristics of estrogen receptors present in uterine nuclei at various times after hormone administration.

Our interest in this area was stimulated by a provocative series of reports which raised the interesting possibility that different physiological responses of the uterus to estrogens might result from the nuclear interactions of estrogen receptors at different times after hormone administration (Anderson et al., 1972a, 1973, 1975). It therefore seemed important to us to attempt to define the nuclear retention patterns of uterine estrogen receptors, and to determine if receptors were modified in uterine nuclei.

Materials and Methods

Animals. Immature female rats (20–21 days old) were obtained from Texas Inbred Mice Co., Houston, Texas. Tritiated estradiol (48 Ci/mmol, New England Nuclear) or unlabeled estradiol (Schwarz/Mann) were given intraperitoneally in a volume of 0.5 ml of saline containing 5% ethanol. At the indicated times the animals were sacrificed by decapitation and the uterus removed and stripped of adhering fat and mesentery.

Isolation of Nuclei. Uteri were homogenized in 0.01 M Tris, pH 7.4, containing 1.5 mM EDTA[1] (TE buffer) using a ground-glass homogenizer. Crude nuclear-myofibrillar pellets were then obtained by centrifugation at 800*g* for 10 min. For the studies of total nuclear content of radioactive

† From the Department of Pharmacology, The University of Texas Medical School at Houston, Houston, Texas 77025. *Received June 9, 1975.* Supported by NIH Grant HD 08615 and The Faith Foundation. A preliminary report of this work was presented at the 6th Annual Gulf Coast Molecular Biology Conference, Corpus Christi, Texas, January 24–26, 1975.

[1] Abbreviations used are: E_2, estradiol; EDTA, ethylenediaminetetraacetic acid; TE buffer, Tris-EDTA.